Selective Cesium Adsorptive Removal on Using Crosslinked Tea Leaves

Dan Yu [1], Shintaro Morisada [1], Hidetaka Kawakita [1], Keisuke Ohto [1,*], Katsutoshi Inoue [1], Ximing Song [2] and Guolin Zhang [2]

[1] Department of Chemistry and Applied Chemistry, Faculty of Science and Engineering, Saga University, Saga 840-8502, Japan
[2] College of chemistry, Liaoning University, Shenyang 110036, China
* Correspondence: ohtok@cc.saga-u.ac.jp; Tel./Fax: +81-952-28-8669

check for updates

Abstract: To remove the radioactive cesium from the polluted environment, tea leaves were chosen as cheap, and abundantly available environment-friendly bio-adsorbents to investigate the alkali metals adsorption. Fresh and used tea leaves (FT and UT) were found to have high efficiency and selectivity for cesium adsorption, after the crosslinking with concentrated sulfuric acid. Calculation of the proton-exchanged amount suggested adsorption mechanism of three alkali metals on crosslinked tea leaves involve a cationic exchange with a proton from the hydroxyl groups of the crosslinked tea leaves, as well as coordination with ethereal oxygen atoms to form the chelation. Further, considering the practical application of the polluted water treatment, the competitive adsorption of Cs^+ and Na^+ ions was investigated by the batch-wise method and column chromatography separation. Unlike the conventional ion exchange and chelate resins with less selectivity for Cs^+ coexisting cations, both crosslinked fresh tea leaves (CFT) and crosslinked used tea leaves (CUT) exhibited Cs selectivity over Na. In addition, batch adsorption studies revealed that the cesium adsorptions were driven by the Langmuir isotherm model; the capacity of both crosslinked tea leaves for cesium adsorption was determined to be around 2.5 mmol g^{-1}. The adsorption capacities are sufficiently higher in comparison with those of synthetic polymers, inorganic ion-exchangers, and other bio-adsorbents.

Keywords: biomass wastes; cesium selectivity; ion-exchange; adsorptive removal

1. Introduction

Cesium, the most active alkaline metal, is generally used in the photoelectric cells and various optical instruments [1]. Natural cesium mainly exists as ^{133}Cs, also slightly inclusive of other 11 major radioactive isotopes. Three among them were concerned about the radioactive hazards because of their long-term of half-life, ^{134}Cs (2.1 years), ^{135}Cs (2.3 million years), ^{137}Cs (30.17 years) [2]. Radioactive ^{137}Cs, as a representative fission product of uranium^{235}, has been specifically increased the utilization in a nuclear power plant. The Fukushima Daiichi nuclear power plant accident at Okuma, Fukushima, Japan, produced massive hazardous nuclear waste in the form of dust into the atmosphere. The released nuclear waste contained hazardous radioactive cesium, which was eventually adsorbed onto soil and was contaminated into the groundwater, nearby seawaters, etc. The cesium and other radioactive contaminated waters reached into the human body through the food chain, can cause several unhealthy effects, such as cancers, for longer terms. Therefore, the method and technique to reduce cesium pollution have been the utmost required.

For cesium recovery, general methods, solid adsorption, and solvent extraction, have been so far applied. Some extractants exhibit remarkable efficiency for cesium (I) extraction due to their specific macrocyclic structures [3–5], despite having some disadvantages such as the use of

flammable and undesirable organic solvents. Metal ion adsorption either on the surface or inner of adsorbents from aqueous solution can, therefore, an alternative method without employing toxic extractants and diluents is recommended. In addition to the synthetic adsorbents, such as organic compounds and polymers [6,7], the adsorbents obtained from the nature like resources-minerals and bio-adsorbents [8,9], with a simple modification, less pollution, and most importantly low-cost, provide the valuable way for cesium recovery.

Recently, because of the characteristics of environmental friendliness and a large wealthy resource of adsorbents, the studies on metal adsorption using biomass adsorbents has been focused for several years [10–12]. The presence of various active functional groups, like amino, hydroxyl, carboxylic acid, and carbonyl groups, etc. in adsorbents makes them available for chelation or complexation with metal ions. As the effective and cheaper materials of bio-adsorbents, tea leaves have high yield and consumption in the world. In addition, the chemical composition of tea leaves are constituted of alkaloids, proteins, amino acids, carbohydrates, polyphenols, chlorophyll, volatile compounds, fluoride, minerals, trace elements, and other undefined compounds [13,14]. Remarkably, the phenolic components in tea leaves have more than 10 kinds of structures. In the green tea leaves, flavan-3-ol and flavonols are the main substances. The black tea, produced by fermentation of green tea leaves, mainly contains gallic acid derivatives, flavonols, and thearubigins [15,16]. Therefore, the presence of these groups provides the potential benefit to metal recovery by the ion-exchange or complexation with the active groups. It was reported that Cr (VI) adsorption on tea waste/Fe_3O_4 composite and the mechanism involved electrostatic attraction, reduction process, ion-exchange, and surface complexation, etc. [17]. In addition, Wan et al. reported the adsorption of divalent heavy metals, Pb (II), Cd (II), and Cu (II), adsorption was based on ion-exchange with the phenolic hydroxyl groups [18]. The successful removal of heavy metals on using tea leaves implies their ability for divalent metal adsorption. It is indirectly implied that they may even have a potential for the monovalent metal ions adsorption by simple modification, like decrease the number of hydroxyl groups. To figure out the relevance of the assumption and estimation of adsorption ability, crude and crosslinked tea leaves were employed to adsorption of alkali metals.

Hence, in this present work, the phenol groups on fresh and used tea leaves were independently crosslinked to form ether groups by condensation assisted by catalysis of concentrated sulfuric acid. Both the crosslinked tea leaves were continuously applied to other alkali metals (Na and K) adsorption to elucidate the adsorption mechanism. Furthermore, the potential recovery of Cs on two types of crosslinked tea leaves by the batch method and column chromatography were assessed.

2. Materials and Methods

2.1. Reagents

Analytical grade alkali metal chlorides (CsCl, KCl, and NaCl) and alkali metal hydroxide (CsOH, KOH, and NaOH), purchased from Wako Reagent Co., Ltd., Tokyo, Japan, were used to prepare sample solutions. The concentrated sulfuric acid and hydrochloric acid were also purchased from Wako Chemicals. The fresh and used tea leaves were kindly supplied by Ochachamura Mine Tea MFG., Co., Uresino-city, Saga, Japan.

2.2. Preparation Method for Adsorbents

The used tea leaves were stored in a freezer to prevent from getting mold. As the pre-treatment, the leaves were dried in an oven for 72 h at 60 °C. For crosslinking, 15.0 g fresh and used tea leaves were stirred in 50 cm^3 concentrated sulfuric (18.4 mol dm^{-3}) acid at 90 °C for 20 h. The mixtures were cooled down to room temperature and soaked into 500 cm^3 deionized water. After the filtration, the product was packed into the glass column and continuously washed with deionized water until the pH of the solution became neutral. Then, the washed product was dried at 60 °C for 48 h. Finally, the obtained cake was crushed and ground, then sieved through 150 μm mesh to keep the uniform size. The images

and the micrographs of tea leaf surfaces before and after the crosslinking were measured by scanning electron microscope (SEM) and X-ray diffraction (XRD).

2.3. Batch Adsorption Experiments

The pH of the alkali metal solution was adjusted by mixing 1.0 mM MOH (alkali metal hydroxide) solution and 1.0 mM MCl (alkali metal chloride) containing 0.10 M HCl solution. The solution of the time dependency test was used by the alkali metal solution of pH 2.6. Fifty milligrams adsorbents were added to 10 cm^3 of all the metal samples. Then, the mixture was shaken at 150 rpm at 30 °C for 24 h. After filtration, the metal concentration of an aqueous solution was measured by atomic absorption spectrophotometer (AAS, Shimadzu model AA-6650, Kyoto, Japan), and IR spectra of the adsorbents were measured after drying. For the maximum adsorption capacity test, the different concentrations of alkali metal solution were prepared by the direct addition of different amounts of MCl powder into 10.0 mM MOH solution. The solution concentration lower than 10.0 mM was diluted using deionized water.

2.4. Column Adsorption Experiment

The column chromatographic setup was provided by the peristaltic pump (IWAKI PST-100N, Tokyo, Japan), connected to 8 mm diameter glass column in which glass beads, cotton, and 0.15 g (volume is 0.515 cm^3) adsorbents were successively packed. Deionized water was first passed through the column, followed by water was exchanged with the coexisting metal ions: Cs$^+$ and Na$^+$, at the constant flow rate, of 5.52 cm^3 h^{-1} for crosslinked fresh tea leaves (CFT) and 5.85 cm^3 h^{-1} for crosslinked used tea leaves (CUT), respectively. The concentrations of Cs$^+$ and coexisting Na$^+$ in solution adjusted to 1.84 and 2.68 mM for the experiment using CFT, while the concentrations of Cs$^+$ and Na$^+$ were 1.80 and 2.39 mM for using CUT. The pH values of both feed solutions were adjusted to 8.9. At the equilibrium, pH value was around 7.7 (CFT) and 7.4 (CUT), and they were close to the neutral solution and similar to the batch experimental pH value. Finally, the solution passed through the column was collected at a constant interval by the fraction collector (BIORAD Model 2110 Fraction Collector, Berkeley, California, USA). At a fixed flow rate, the volumes of every samples collected were calculated and the metal concentrations of every sample were measured by AAS to obtain mol amount of the adsorbed metal. At the saturated state of the adsorption, the sum of the molar mass of the adsorbed metal divided by the mass of the adsorbent corresponded to adsorption capacity. After the adsorption reached a breakthrough, the adsorbed metal ions were eluted with HCl solution (pH 1.9) by using the peristaltic pump at the constant flow rate. The eluted flow rates for the experiments using CFT and CUT were adjusted to 4.68 and 4.62 cm^3 h^{-1}. The eluted solutions were collected by the same procedure as a breakthrough test.

2.5. Evaluation of Adsorption Measurements

The alkali metal concentrations of all solutions were measured by AAS. The pH value of the sample solution was measured by a pH meter (DKK-TOA model HM-25G). The FT-IR spectra of all the samples were measured in the range of 4000–400 cm^{-1} wave number with FTIR spectrophotometer (JASCO model FTIR-410 spectrophotometer) by using the KBr pellet method. The micrographs of the metal loading materials were taken by SEM. The XRD images of the tea leaves and crosslinked tea leaves were also measured.

The adsorption percentage (%) and the amount of alkali metal ions adsorbed on all the adsorbents (q, mmol g^{-1}) were calculated by the following formularies:

$$\text{Adsorption percentage (\%)} \ = \ \frac{C_i - C_e}{C_i} \times 100$$

$$q \ = \ \frac{C_i - C_e}{W} \times V_M$$

where C_i (mmol dm^{-3}) and C_e (mmol dm^{-3}) are the initial and equilibrium concentrations of metal ions, respectively. V_M is the volume (dm^3) of sample solution, and W is the weight of the adsorbent (g).

3. Results and Discussion

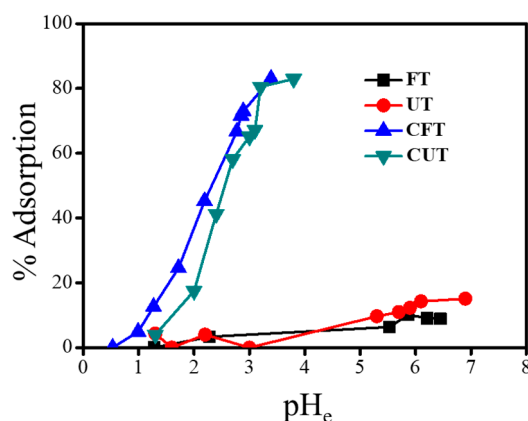### 3.1. Adsorption of Cesium Ions on Crude and Crosslinked Tea Leaves

The SEM images of tea leaves before and after crosslinking are shown in Figure 1a–d. The used tea leaves (UT) were once soaked in hot water for a beverage before the experiment, and then they were dried again. These pretreatments led to the appearance of more folding layers than those of on fresh tea leaves (FT). After the crosslinking, the surfaces of both materials became smooth. That phenomenon indirectly showed that the impure substances on tea leaves were removed by the crosslinking. The XRD images of materials metal loading samples are shown in Figure S1a,b. The result showed the subtle but important information on supporting crosslinking. Four tea leaves have an amorphous structure without any sharp peaks, but with broad folding points except UT. The UT had a peak, while CUT had no peaks. It is good evidence that UT was successfully crosslinked. By careful observation, the folding points of the crosslinked materials were slightly shifted to the higher angles than those of the original ones. It means that lattice spaces of the crosslinking materials became narrower than those of the original ones. The crosslinking formed ethereal bonds by condensation of phenolic groups, and consequently, the distance between molecules became closer. Therefore, it is also good evidence that the materials were successfully crosslinked.
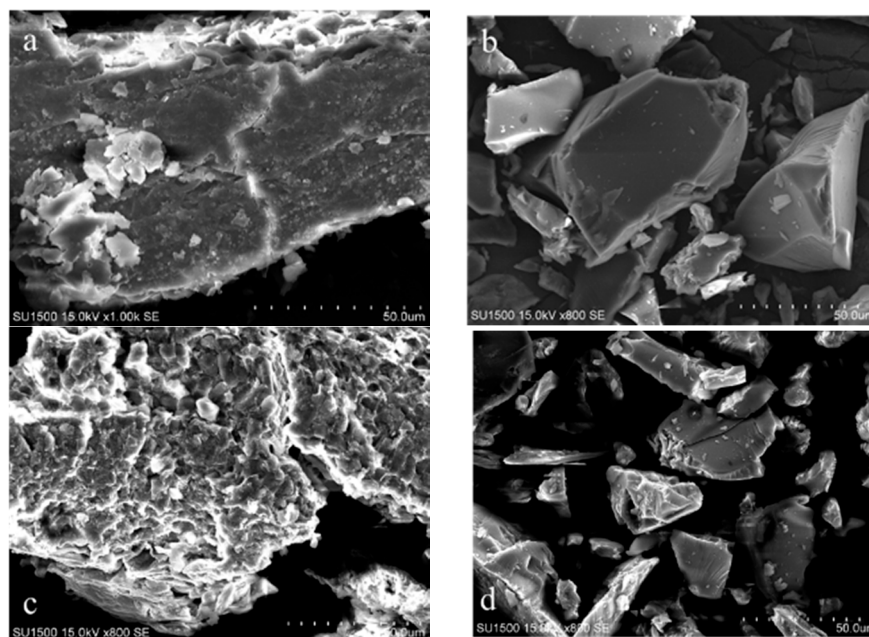
Figure 1. SEM images of tea leaves before and after the crosslinking, (**a**) fresh tea leaves (FT), (**b**) crosslinked fresh tea leaves (CFT), (**c**) used tea leaves (UT), and (**d**) crosslinked used tea leaves (CUT).

Adsorption of Cs$^+$ ions on crude and crosslinked tea leaves at different pH values is shown in Figure 2. Both of crosslinked adsorbents, CFT and CUT, showed the better performance of Cs$^+$ adsorption than FT and UT at various pH values. The heating of crude tea leaves with concentrated sulfuric acid and some polymers, such as cellulose and hemicellulose [19,20], were partly hydrolyzed to the soluble product, as mentioned in the SEM section. With the washing treatment, the removal of a large number of unreacted substances obviously improved the activity of the material. Besides, in the aqueous phase, the alkali metal cations have coordination with water molecules [21,22]. In the Figure, the Cs$^+$ adsorption on both CFT and CUT is sensitively dependent on pH values of aqueous solutions; hence, the adsorption mechanism is related to the ion-exchange. Furthermore, the production of

ether groups through crosslinking could coordinate with Cs^+ ion to replace its coordination with oxygen atoms of water molecules. Therefore, by the function of coordination, Cs^+ was promoted contacting with hydroxyl groups, and the ion-exchange reaction took place. Based on such discussion, the proposed model of Cs^+ adsorption on crosslinked tea leaves is described in the Scheme 1. That is, after the crosslinking, the phenolic hydroxyl groups were partially converted to ether groups. The crosslinked adsorbents still provided ion-exchangeable hydroxyl groups, and consequently, metal adsorption was driven by the ion-exchange mechanism. Meanwhile, the adsorbents also provided coordinatively-active ethereal oxygen atoms for the dehydration of metal ions and attached to these metal cations on their surface.


Figure 2. Adsorption of Cs^+ ions on crude and crosslinked tea leaves as a function of equilibrium pH, adsorbent weight = 0.05 g, solution volume = 10.0 cm^3, $[Cs^+]_i$ = 1.0 mM, shaking time = 24 h.

Scheme 1. Modification of tea leaves and Cs adsorption process in the aqueous phase.

3.2. Effect of Shaking Time on Adsorption of Alkali Metal Ions

Due to the low adsorption potential of crude FT and UT, the alkali metal ion adsorption on crosslinked adsorbents was only of focus on the subsequent experiments. The effect of shaking time on adsorption of alkali metal ions on the crosslinked adsorbents is shown in Figure 3a,b. Cesium has the largest ionic radius and consequently has the lowest charge density. Adsorption of alkali metal ions on crosslinked adsorbents was sufficiently fast to reach quantitative adsorption within 6 h. Thus, it was found that crosslinked adsorbents exhibited a high effect on the adsorption of alkali metal ions.
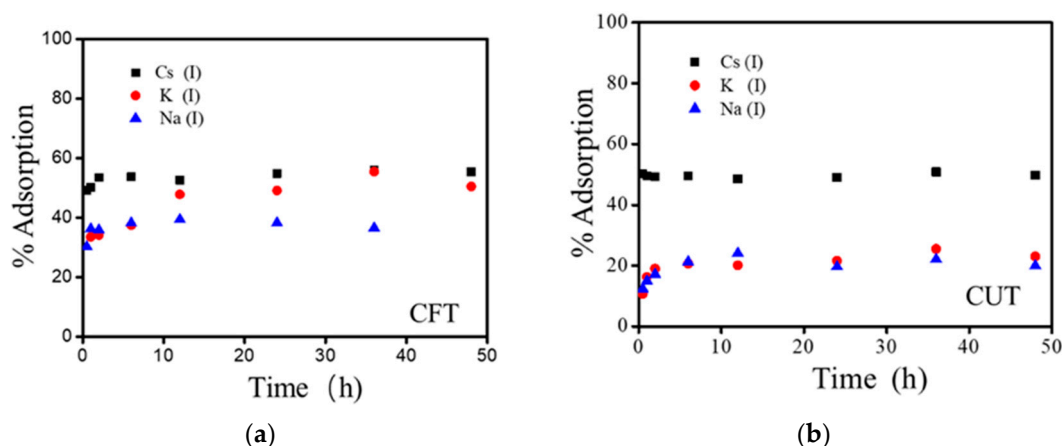
Figure 3. Effect of time of alkali metal ion adsorption on (**a**) crosslinked fresh tea leaves (CFT) adsorbents and (**b**) crosslinked used tea leaves (CUT) adsorbents, adsorbent weight = 0.05 g, solution volume = 10.0 cm^3, [M$^+$]$_i$ = 1.0 mM, pH$_e$= 2.5, shaking time = several hours.

3.3. Effect of pH on Adsorption of Alkali Metal Ions

For further study on the mechanism of Cs$^+$ ion adsorption on crosslinked tea leaves and other alkali metal (Na and K) ions, adsorption was investigated at different pH range (1–11) as well.

The effect of equilibrium pH (pH$_e$) on adsorption percentage is shown in Figure 4a,b. The fitting curves theoretically drawn in the figures are discussed later. As Figure 4 shows, Cs$^+$ was slightly selectively adsorbed on both crosslinked tea leaves over other smaller two ions. A monovalent metal ion with smaller ionic radius has higher charge density and consequently has higher hydration energy than that with a larger radius. Therefore, larger Cs$^+$ was easily dehydrated than smaller K$^+$ or Na$^+$ and preferably adsorbed among alkali metal ions.

The adsorption percentage was increased with increasing pH value, and the pH value was dramatically dropped after the adsorption because protons were released from crosslinked adsorbents and ion-exchanged with a metal ion. It is reasonable that the adsorption reaction of alkali metal ions is driven by the cationic exchange. The adsorption equation is written as follows:

$$M^+ + ROH \overset{K_{ad}}{\rightleftharpoons} ROM + H^+$$
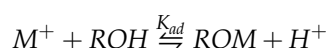
where M and *ROH* represent alkali metal and active polyphenolic sites of adsorbents in crosslinked tea leaves, respectively, and K_{ad} represents the equilibrium adsorption constant of alkali metal ion.

As that equation indicates that one alkali metal cation was adsorbed on the phenolic group, and one proton was released from the phenolic hydroxyl group at the same time.

The calculated equilibrium adsorption constant (K_{ad}) of alkali metal ion from the reactional equation is represented as following, where η represents the amount of substance (mol).

$$K_{ad} = \frac{\eta_{ROM}\,\eta_{H^+}}{\eta_{ROH}\,\eta_{M^+}}$$

Here, the ratio of metal concentration between solid and aqueous phases is simply defined as the distribution ratio (*D*). The obtained mole ratio between the raw adsorbents and adsorbed metal adsorbents (η_{ROM}/η_{ROH}) is as following description:

$$D = \frac{q}{C_e} = \frac{(C_i - C_e)V_m}{C_e\,m_{ROH}}$$

$$\frac{\eta_{ROM}}{\eta_{ROH}} = \frac{(C_i - C_e)\,V_M}{m_{ROH}/M_{ROH}}$$

where the M_{ROH} represents the total molecular molar mass (mol kg^{-1}) of adsorbents and m$_{ROH}$ represents the weight (kg) of adsorbents.

After those formula derivations, distribution ratio was taken logarithm, and obtained value of log$D$ is as follow.

$$\log D = \log K_{ad} - \log M_{ROH} + \mathrm{pH}_e$$

The relationship between log$D$ and equilibrium pH value (pH$_e$) is linear. The effect of equilibrium pH on distribution ratio is shown in Figure 5a,b. All plots lie on the straight lines with certain slopes listed in Table 1. All of the slopes are close to one, which adequately indicates that all adsorption reactions of alkali metal ions are driven by the cationic exchange, namely, one proton was released by loading one cation. Although used tea leaves supplied after the use for beverage, it was expected that water-soluble molecules dissolved and lost before the crosslinking. The slope of crosslinked tea leaves was close to one as well, which means that the little number of ether groups in tea leaves hardly affected Cs$^+$ adsorption.

Table 1. Calculated slope value of alkali metal ions based on the equations.

Adsorbent	Cs$^+$		K$^+$		Na$^+$	
	Slope	R^2	Slope	R^2	Slope	R^2
CFT	0.822	0.9863	0.858	0.9953	0.831	0.9919
CUT	0.997	0.9795	0.861	0.9860	0.780	0.9510

CFT and CUT respectively represents the crosslinked fresh and use tea leaves.

The intercept of the fitting equation in Figure 5 represents the logarithm value of the ratio of K_{ad} to M_{ROH} (log K_{ad}/M_{ROH}), and "a" was used for instead of that value at the following description. Comprehensively, the relation between adsorption percentage (*Ad%*) and equilibrium pH value (pH$_e$) is deduced as follows:

$$Ad = \frac{C_i - C_e}{C_i} = 1 - \frac{C_e}{C_i}$$

$$\frac{Ad}{1 - Ad} = \frac{K_{ad} m_{ROH}}{V_M M_{ROH}[H^+]} = \frac{a\, m_{ROH}}{V_M[H^+]}$$

$$Ad\% = \frac{100\, a\, m_{ROH}}{V_M\, 10^{-pHe} + a\, m_{ROH}}$$

The deduced relation was reflected to plot the fitting curve in Figure 4, each curve of alkali metal ions was calculated with the value of the respective slope in Table 1. The logarithm value of the ratio of K_{ad} and M_{ROH} (replaced as a) results by the calculation of fitting equation. All the R square values of linear lines drawn in Figure 4 are higher than 0.99. All experimental data of adsorption percentage in Figure 4 are very reliably close to the calculated curve.
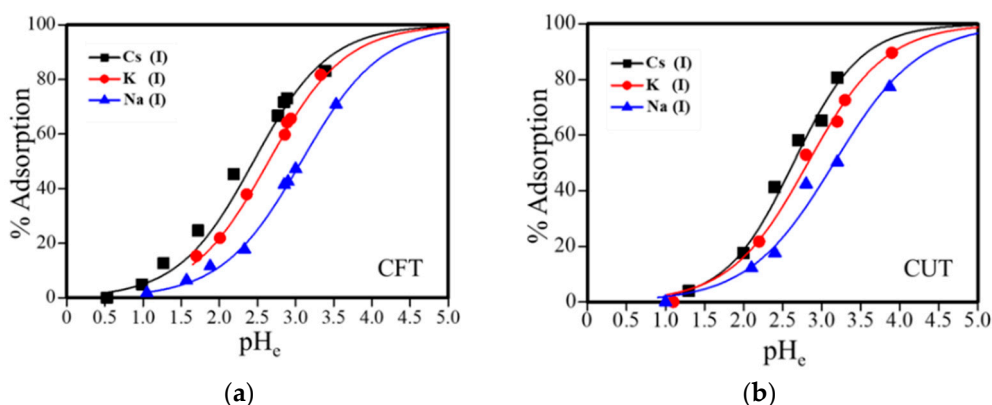
Figure 4. Effect of pH dependency on adsorption of alkali metal ions on (**a**) crosslinked fresh tea leaves (CFT) adsorbents and (**b**) crosslinked used tea leaves (CUT) adsorbents at 303K, adsorbent weight = 0.05 g, solution volume = 10.0 cm^3, [M$^+$]$_i$ = 1.0 mM each, shaking time = 24 h.
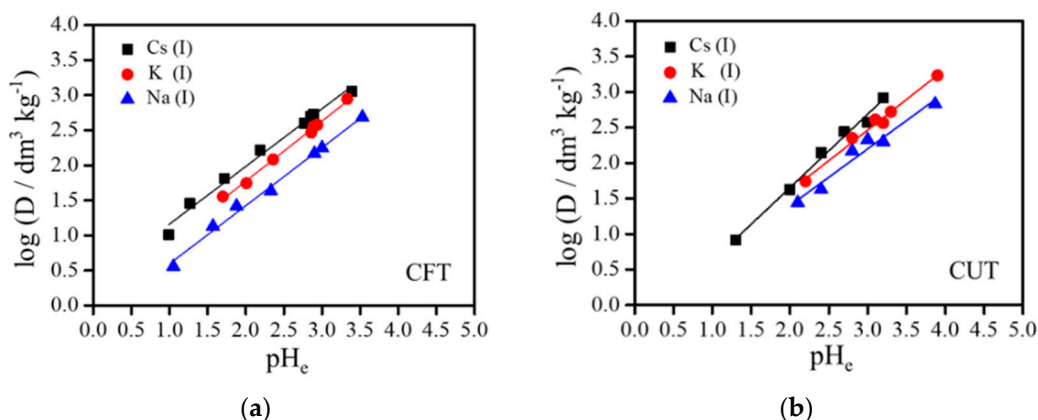
Figure 5. Effect of pH$_e$ value on distribution ratio of alkali metal ion at 303K, (**a**) crosslinked fresh tea leaves (CFT) adsorbents and (**b**) crosslinked used tea leaves (CUT) adsorbents, adsorbent weight = 0.05 g, solution volume = 10.0 cm^3, [M$^+$]$_i$ = 1.0 mM each, shaking time = 24 h.

3.4. Adsorption Isotherms of Na$^+$ and Cs$^+$ Ions on CFT and CUT Adsorbents

Naturally, the large existence of sodium ions leads to unavoidably the large amount of competitive ions containing in the polluted water. Hence, the adsorption isotherms for Na$^+$ and Cs$^+$ ion on CFT and CUT adsorbents at similar pH$_i$ (around 11) condition were investigated, as shown in Figure 6a,b, respectively. The adsorption amounts of adsorbents for Na$^+$ and Cs$^+$ ions increased with the increase of initial metal concentration and reached the maximum loading capacity. The results show that metal adsorption is classified into the Langmuir models [23]:

$$q_e = \frac{q_m * b * C_e}{1 + b * C_e} = \frac{q_m * C_e}{1/b + C_e}$$

where q$_e$ is the adsorbed amount at equilibrium (mmol g^{-1}); q$_m$ is the maximal adsorption capacity (mmol g^{-1}); b is the Langmuir constant related to the adsorption energy (dm^3 mmol^{-1}).
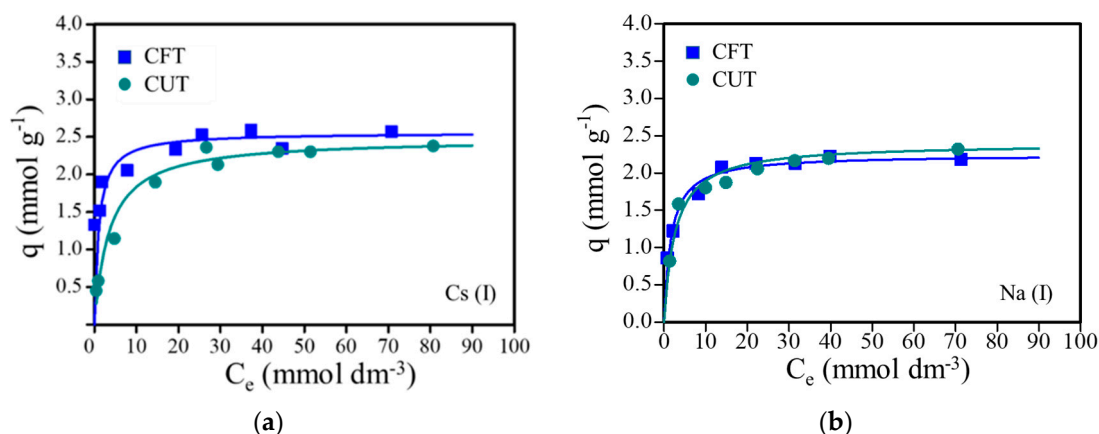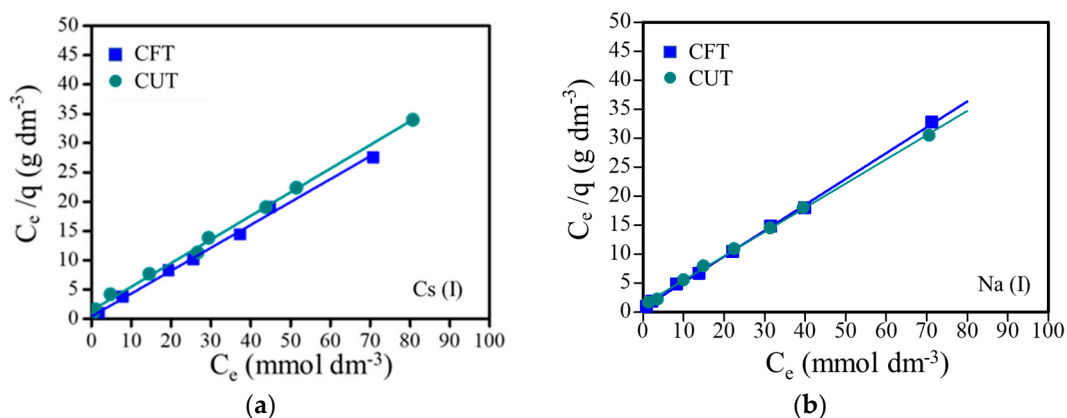
Figure 6. Adsorption isotherms: (**a**) Cs$^+$ ion on crosslinked fresh tea leaves (CFT) and crosslinked used tea leaves (CUT) adsorbents, (**b**) Na$^+$ ion on CFT and CUT adsorbents, adsorbent weight = 0.05 g, solution volume = 10.0 cm^3, pH$_e$ = 7.0 ± 1.0 (Cs$^+$) and 7.5 ± 0.5 (Na$^+$), shaking time = 24 h.

As per the experimental data, the maximal adsorption capacities of Cs$^+$ and Na$^+$ on CUT adsorbents are 2.3 and 2.4 mmol g^{-1}, while those on CFT adsorbent are 2.5 and 2.2 mmol g^{-1}. To confirm the validity of the obtained maximum adsorption capacities, Langmuir formula was linearly transformed and described as follow:

$$\frac{C_e}{q_e} = \frac{1}{q_m\, b} + \frac{C_e}{q_m}$$

The maximum adsorption capacity obtained from linear relationship between $C_e\, q^{-1}$ and C_e. Figure 7a,b show transformed Langmuir adsorption isotherm of Cs$^+$ and Na$^+$ ions on CFT and CUT adsorbents.

Figure 7. The Langmuir isotherm kinetic models: (**a**) Cs$^+$ ion adsorption on crosslinked fresh tea leaves (CFT) and crosslinked used tea leaves (CUT) adsorbents, (**b**) Na$^+$ ion on CFT and CUT adsorbents, adsorbent weight = 0.05 g, solution volume = 10.0 cm^3, pH$_e$ = 7.0 ± 1.0 (Cs$^+$) and 7.5 ± 0.5 (Na$^+$), shaking time = 24 h.

The Langmuir parameters and maximal adsorption capacities can be calculated from the intercept and the slope of the straight line by linear regression analysis, and the obtained values are listed in Table 2. The R^2 values of both adsorbents are higher than 0.99, and it is also verified that adsorption is governed by the Langmuir model. On the other hand, the maximal capacities of Cs$^+$ and Na$^+$ on CUT adsorbents are 2.48 and 2.40 mmol g^{-1}, while those on CFT adsorbents are 2.56 and 2.25 mmol g^{-1}. Those values, corresponding to the values obtained from Figure 6a,b, particularly confirm the reliability of values. In addition, the Cs$^+$ adsorption capacities on CUT and CFT adsorbents were compared with those obtained by using other adsorbents with the batch method as listed in Table 3. As a comparison,

the Cs$^+$ capacities on both types of crosslinked adsorbents are sufficiently high. Especially for the used tea leaves, they are much economical than the fresh tea leaves but have a similar capacity on Cs$^+$ ion adsorption as CFT.

Table 2. Langmuir isotherm constants for the adsorption of Na$^+$ and Cs$^+$ on adsorbents.

	CUT Adsorbent			CFT Adsorbent		
	Q$_m$ (mmol g^{-1})	B (dm^3 mmol^{-1})	R^2	Q$_m$ (mmol g^{-1})	B (dm^3 mmol^{-1})	R^2
Na$^+$	2.40	0.6431	0.999	2.25	0.3182	0.999
Cs$^+$	2.48	0.2802	0.997	2.56	0.9950	0.996

CFT and CUT respectively represents the crosslinked fresh and use tea leaves.

Table 3. Comparisons of adsorption capacities of present adsorbents with various kinds of other adsorbents for Cs$^+$ ion reported in the literature.

| Adsorbent	Adsorption Capacity (mmol g^{-1})	pH	Temperature(K)	Reference
Layered metal sulfide (KMS−1)	1.70	≈7.0 (pH$_e$)	298	[24]
Sericite	0.050	5.0 (pH$_i$)	298	[25]
RIP of clay minerals	0.250	7.0 (pH$_i$)	*	[26]
Prussian blue	1.254	Water	298	[27]
Biomass of marine algae	0.248	5.5 (pH$_i$)	303	[28]
Arca shell biomass	0.036	5.5 (pH$_i$)	298	[29]
CUT	2.48	7.0 ± 1.0 (pH$_e$)	303	Present work
CFT	2.56	7.0 ± 1.0 (pH$_e$)	303	Present work

* Temperature was not mentioned in the article, CFT and CUT respectively represents the crosslinked fresh and use tea leaves.

3.5. Chromatography Separation of Cs$^+$ over Na$^+$ Ion Using Crosslinked Tea Leaves

Based on the investigation of adsorption isotherm of Na$^+$ on crosslinked tea leaves by the batch experimental result, the high adsorption capacity of Na$^+$ may cause competition of Cs$^+$ adsorption in the co-existing solution. Hence, the essential investigation on adsorption of Cs$^+$ in excessive Na$^+$ solution by column chromatography technique was studied.

Figure 8a,b show the breakthrough profiles of Cs$^+$ and Na$^+$ adsorption on CFT and CUT, respectively. The metal selectivity given here was followed by the result shown in Figure 4a,b.

Furthermore, adsorption capacities of the adsorbents towards Cs$^+$, as listed in Table 4, are much higher than that of Na$^+$. For CFT adsorbents, the adsorption capacities of Cs$^+$ and Na$^+$ were evaluated as 0.992 and 0.528 mmol g^{-1}. For CUT adsorbents, the capacities of Cs$^+$ and Na$^+$ were 0.804 and 0.491 mmol g^{-1}. The selectivity of CUT and CFT towards Cs$^+$ is jointly decided by the lower hydration energy and stable coordination. The CFT and CUT adsorbents still sufficiently exhibited high ability to remove Cs$^+$ from co-existing solution.
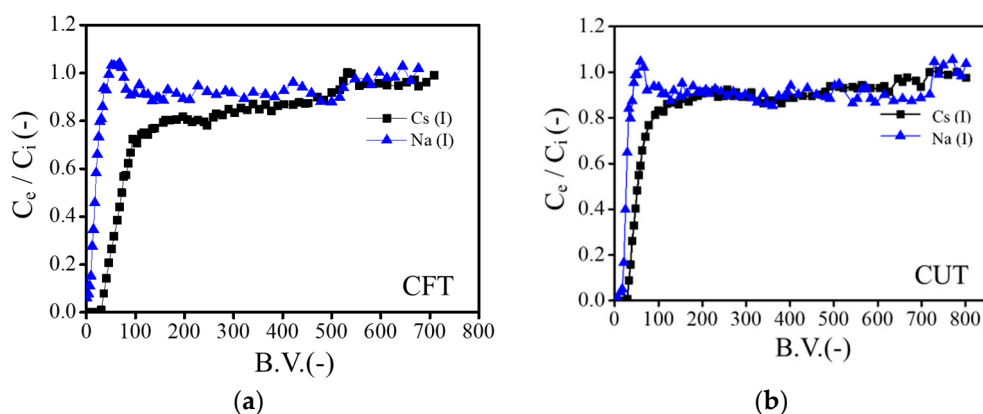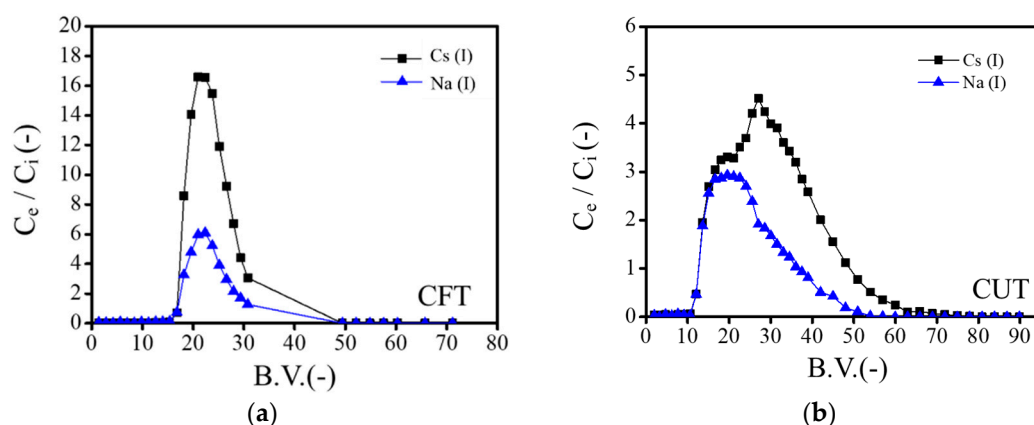
Figure 8. Breakthrough profiles of Cs^+ and Na^+ ions upon passing the column packed with (**a**) crosslinked fresh tea leaves (CFT) adsorbents and (**b**) crosslinked used tea leaves (CUT) adsorbents, pH_e = 7.7 (CFT) and 7.4 (CUT), weight of adsorbents= 0.15 g (0.515 cm^3), $[Cs^+]_i$ = 1.84 mM (CFT), 1.80 mM (CUT), $[Na^+]_i$ = 2.68 mM (CFT), 2.39 mM (CUT), flow rate = 5.52 cm^3 h^{-1} (CFT) and 5.85 cm^3 h^{-1} (CUT).

Table 4. Separation and removal of Cs^+ from the mixture of Na^+ ions.

	CUT Adsorbent			CFT Adsorbent		
	Adsorbed (mmol g^{-1})	Eluted (mmol g^{-1})	% Recovery	Adsorbed (mmol g^{-1})	Eluted (mmol g^{-1})	% Recovery
Na^+	0.491	0.484	98.57	0.528	0.497	94.13
Cs^+	0.804	0.716	89.05	0.992	0.951	95.78

CFT and CUT respectively represents the crosslinked fresh and use tea leaves.

After the saturation of the adsorbent bed, it was eluted by HCl solution with pH value adjusted to 1.9 to recover the adsorbed metal ions, and the elution profiles are shown in Figure 9a,b. It was found that massive metal ions were immediately released in a short period. Finally, all metal ions were eluted, as listed in Table 4. The high efficiency of recoveries implies that tea leaves have the potential for the contaminated water treatment, especially the used tea leaves.


Figure 9. Elution profiles of the adsorption of Cs^+ and Na^+ ion on (**a**) crosslinked fresh tea leaves (CFT) adsorbents and (**b**) crosslinked used tea leaves (CUT) adsorbents with HCl solution, pH = 1.9, flow rate = 4.68 cm^3 h^{-1} (CFT), 4.62 cm^3 h^{-1} (CUT).

3.6. Fourier-Transfer Infrared Analysis

For the further study on the adsorption sites in adsorbents for alkali metal adsorption, FT-I spectra of series of the adsorbents before and after the metal adsorption were studied, as shown in

Figure 10a,b. Either crude or crosslinked tea leaves had broad bands at 3310–3430 cm^{-1}, which were assigned as phenolic *O-H* stretching. CFT and CUT were obtained by partial crosslinking of hydroxyl groups of FT and UT by the condensation assisted by catalysis of concentrated sulfuric acid. Hence, after the crosslinking, the peaks of *O-H* became lower but still existed. While, they became slightly wider and shifted to a lower frequency, due to the formation of a hydrogen bond between hydroxyl groups and formed ether oxygen atoms. Besides, the broken hydrogen bonds, as well as ion-exchange between Cs$^+$ and proton, led to the shifted peaks with slight sharper shape, after Cs$^+$ adsorption. The peaks located at 1600 cm^{-1} are identified as the stretching vibrations of *C = C* groups derived from benzene rings. The effect of crosslinking was also reflected on the shift of *C = C* peaks on CFT and CUT. The observation of effect from formed hydrogen and ether bonds to changes in peaks in FT-IR could be supported on obtained analysis of shrank spatial distance in XRD figures as well.

(**a**) (**b**)
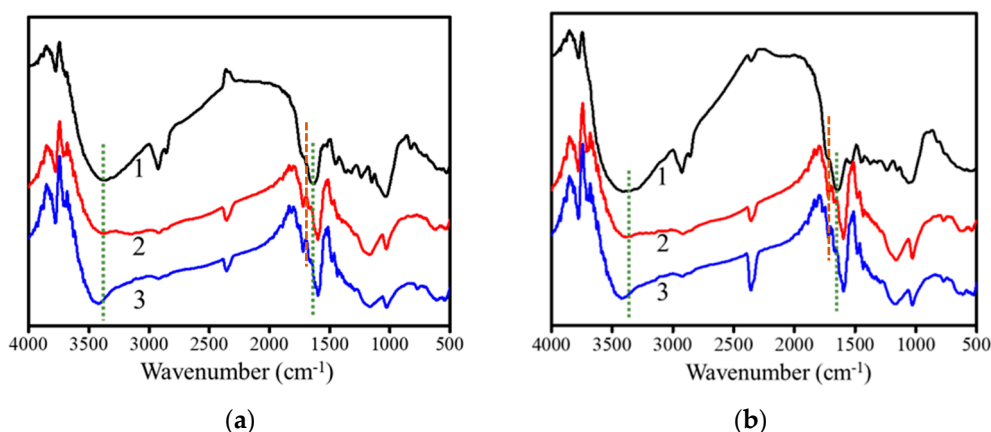
Figure 10. FT-IR spectra of adsorbents, (**a**) 1 FT, 2 CFT, 3 CFT- adsorbed Cs$^+$ and (**b**) 1 UT, 2 CUT, 3 CUT-adsorbed Cs$^+$. FT: fresh tea leaves; CFT: crosslinked fresh tea leaves; UT: used tea leaves; CUT: crosslinked used tea leaves.

In addition, the medium bands around 2930 and 2850 cm^{-1} of two types of crude tea leaves are attributable to *C-H* stretching frequencies. After crosslinking, the degradation of some polymers led to the weaker intensity of C-H on CFT and CUT. The new moderate peaks appeared at 1160 cm^{-1} on CFT and CUT, belonging to *C-O-C* stretching vibrations, and they were caused by the formation of C-O-C linkages produced from the condensation reaction of hydroxyl groups. Furthermore, the ethereal peaks of CFT and CUT were slightly shifted to 1180 cm^{-1} after the Cs$^+$ adsorption. This was caused by the coordination of ethereal oxygen atoms to Cs$^+$.

The ether groups coordinated with Cs$^+$ and replaced with hydrated water molecules. These results from FT-IR strongly supported that the partial crosslinking of the adsorbents converted hydroxyl groups into ethereal oxygen atoms and easily facilitated dehydration of Cs$^+$ by coordination. Consequently, the adsorption reaction was enhanced not only by proton exchange mechanism but also coordination with ether groups.

4. Conclusions

Both the fresh and used tea leaves, as environmentally friendly bio-sorbents, exhibited the excellent adsorption performance of alkali metal ions by crosslinking with concentrated sulfuric acid. Adsorption reaction of alkali metal cations involved coordination and ion exchange. The coordination of Cs$^+$ with hydrated water molecules in aqueous solution was firstly replaced with the oxygen atom from ether groups, which were formed by the crosslinking of tea leaves. Meanwhile, the dehydrated Cs$^+$ ion was adsorbed by ion-exchange with the proton of hydroxyl groups on crosslinked tea leaves and assisted by coordination with ethereal oxygen atoms. Following the Langmuir model, compared with the maximal capacities of Cs$^+$ ions with the batch method on synthesized chemicals,

minerals, and other bio-adsorbents, those on the crosslinked tea leaves exhibited the superior uptake due to the rich phenolic functional groups. Water-soluble molecules were partially eluted, and such small loss had no suppression to the adsorption capacity of CUT, and it was similar to that of CFT. Some conventional cation resins, such as carboxylic acid resin, have less selectivity for monovalent metals [30–32]. On the contrary, a decreased amount of hydroxyl groups on crosslinked tea leaves attributed to partial crosslinking and could lead to weaker electrostatic interaction between ion-exchange groups and metal ions. Furthermore, formed ethereal oxygen atoms are coordinatively-active for dehydration of monovalent metal ions. Therefore, the crosslinked tea leaves had the ability for Na^+, K^+, Cs^+ adsorptions. The different cationic size determined different hydration energy; hence, the selective separation of Cs^+ in excessive Na^+ solution by using column chromatography found that crosslinked tea leaves exhibited Cs^+ selectivity over Na^+. The elution of the loaded Cs^+ ion was successfully achieved with a low concentration of the acidic solution in a short period. Even used tea leaves exhibited comparable adsorption behavior to the fresh ones after crosslinking. Low cost and environmentally friendly adsorbents were easily prepared and could be potential candidates for cesium removal from the polluted solution.

Supplementary Materials: The following are available online at http://www.mdpi.com/2227-9717/7/7/412/s1, Figure S1: X-ray diffraction patterns of (a) fresh and (b) used tea leaves before and after crosslinking, fresh tea leaves (FT), crosslinked fresh tea leaves (CFT), used tea leaves (UT), and (d) crosslinked used tea leaves (CUT).

Author Contributions: D.Y.: did all the experimental operation and manuscript writing. The deduction of the formula was guided from H.K. S.M. participated the measurement and analysis of SEM data. K.I. was the beginner of related research work in our lab and he suggested the modification method. In addition, the analysis of XRD was guided from G.Z. and X.S. The experimental idea, throughout guidance, and revision of manuscript were provided from K.O.

Conflicts of Interest: The authors declare no conflict of interest.

References

1. Peterson, J.; MacDonell, M.; Haroun, L.; Monette, F. *Radiological and Chemical Fact Sheets to Support Health Risk Analyses for Contaminated Areas*; Argonne National Laboratory Environmental Science Division: Washington, DC, USA, 2007.
2. Unterweger, M.P.; Fitzgerald, R. Update of NIST half-life results corrected for ionization chamber source-holder instability. *Appl. Radiat. Isot.* **2014**, *87*, 92–94. [CrossRef] [PubMed]
3. Xu, C.; Wang, J.; Chen, J. Solvent extraction of strontium and cesium: A review of recent progress. *Solvent Extr. Ion Exch.* **2012**, *30*, 623–650. [CrossRef]
4. Shuler, R.G.; Bowers, C.B., Jr.; Smith, J.E., Jr.; van Brunt, V.; Davis, M.W., Jr. The extraction of cesium and strontium from acidic high activity nuclear waste using a purex process compatible organic Extractant. *Solvent Extr. Ion Exch.* **1985**, *3*, 567–604. [CrossRef]
5. Smirnov, I.V.; Stepanova, E.S.; Tyupina, M.Y.; Ivenskaya, N.M.; Zaripov, S.R.; Kleshnina, S.R.; Solov'eva, S.E.; Antipin, I.S. Extraction of cesium and americium with *p*-alkylcalix[8]arenes from alkaline solutions. *Radiochemistry* **2016**, *58*, 329–335. [CrossRef]
6. Zhang, A.Y.; Chai, Z.F. Adsorption property of cesium onto modified macroporous silica-calix[4]arene-crown based supramolecular recognition materials. *Ind. Eng. Chem. Res.* **2012**, *51*, 6196–6204. [CrossRef]
7. Olatunji, M.A.; Khandaker, M.U.; Mahmud, H.N.M.E. Adsorption kinetics, equilibrium and radiation effect studies of radioactive cesium by polymer-based adsorbent. *J. Vinyl Addit. Technol.* **2018**, *24*, 347–357. [CrossRef]
8. Bostick, B.C.; Vairavamurthy, M.A.; Karthikeyan, K.G.; Chorover, J. Cesium adsorption on clay minerals: An EXAFS spectroscopic investigation. *Environ. Sci. Technol.* **2002**, *36*, 2670–2676. [CrossRef] [PubMed]
9. Chen, C.; Wang, J.L. Removal of Pb^{2+}, Ag^+, Cs^+ and Sr^{2+} from aqueous solution by brewery's waste biomass. *J. Hazard. Mater.* **2008**, *151*, 65–70. [CrossRef]

10. Thirumavalavan, M.; Lai, Y.L.; Lee, J.F. Fourier transform infrared spectroscopic analysis of fruit peels before and after the adsorption of heavy metal ions from aqueous solution. *J. Chem. Eng. Data* **2011**, *56*, 2249–2255. [CrossRef]

11. Hu, X.J.; Wang, J.S.; Liu, Y.G.; Li, X.; Zeng, G.M.; Bao, Z.L.; Zeng, X.X.; Chen, A.W.; Long, F. Adsorption of chromium (VI) by ethylenediamine-modified cross-linked magnetic chitosan resin: Isotherms, kinetics and thermodynamics. *J. Hazard. Meter.* **2011**, *185*, 306–314. [CrossRef]

12. QuYang, X.K.; Jin, R.N.; Yang, L.P.; Wen, Z.S.; Yang, L.Y.; Wang, Y.G.; Wang, C.Y. Partially hydrolyzed bamboo (phyllostachys heterocycla) as a porous bioadsorbent for the removal of Pb (II) from aqueous mixtures. *J. Agric. Food Chem.* **2014**, *62*, 6007–6015.

13. Cabrera, C.; Giménez, R.; López, M.C. Determination of tea components with antioxidant activity. *J. Agric. Food Chem.* **2003**, *51*, 4427–4435. [CrossRef] [PubMed]

14. Reto, M.; Figueira, M.E.; Filipe, H.M.; Almeida, C.M.M. Chemical composition of green tea *(Camellia sinensis)* infusions commercialized in Portugal. *Plant Foods Hum. Nutr.* **2007**, *62*, 139–144. [CrossRef] [PubMed]

15. Pereira-Caro, G.; Moreno-Rojas, J.M.; Brindani, N.; Del Rio, D.; Lean, M.E.; Hara, Y.; Crozier, A. Bioavailability of black tea theaflavins: Absorption, metabolism, and colonic catabolism. *J. Agric. Food Chem.* **2017**, *65*, 5365–5374. [CrossRef]

16. Rio, D.D.; Stewart, A.J.; Mullen, W.; Burns, J.; Lean, M.E.J.; Brighenti, F.; Crozier, A. HPLC-MSn analysis of phenolic compounds and purine alkaloids in green and black tea. *J. Agric. Food Chem.* **2004**, *52*, 2807–2815.

17. Fan, S.S.; Wang, Y.; Li, Y.; Tang, J.; Wang, Z.; Tang, J.; Li, X.D.; Hu, K. Facile synthesis of tea waste/Fe_3O_4 nanoparticle composite for hexavalent chromium removal from aqueous solution. *RSC Adv.* **2017**, *7*, 7576–7590. [CrossRef]

18. Wan, S.L.; Qu, N.; He, F.; Wang, M.K.; Liu, G.B.; He, H. Tea waste-supported hydrated manganese dioxide (HMO) for enhanced removal of typical toxic metal ions from water. *RSC Adv.* **2015**, *5*, 88900–88907. [CrossRef]

19. Taherzadeh, M.J.; Karimi, K. Acid-based hydrolysis processes for ethanol from lignocellulosic materials: A review. *Bioresources* **2007**, *2*, 472–499.

20. Farone, W.A.; Guzens, J.E. Method of Producing Sugars Using Strong Acid Hydrolysis of Cellulosic and Hemicellulosic Materials. U.S. Patent 5,562,777, 13 June 1996.

21. Mähler, J.; Persson, I. A study of the hydration of the alkali metal ions in aqueous solution. *Inorg. Chem.* **2012**, *51*, 425–438. [CrossRef]

22. Smith, D.W. Ionic hydration enthalpies. *J. Chem. Educ.* **1977**, *54*, 540–542. [CrossRef]

23. Langmiur, I. The constitution and fundamental properties of solids and liquids. II Liquids. *J. Am. Chem. Soc.* **1917**, *39*, 1848–1906. [CrossRef]

24. Manos, M.J.; Kanatzidis, M.G. Highly efficient and rapid Cs^+ uptake by the layered metal sulfide $K_{2x}Mn_xSn_{3-x}S_6$ (KMS-1). *J. Am. Chem. Soc.* **2009**, *131*, 6599–6607. [CrossRef] [PubMed]

25. Kim, J.O.; Lee, S.M.; Jeon, C. Adsorption characteristics of sericite for cesium ions from an aqueous solution. *Chem. Eng. Res. Des.* **2014**, *92*, 368–374. [CrossRef]

26. Lee, J.; Park, S.M.; Jeon, E.K.; Baek, K. Selective and irreversible adsorption mechanism of cesium on illite. *Appl. Geochem.* **2017**, *85*, 188–193. [CrossRef]

27. Hu, B.; Fugetsu, B.; Yu, H.; Abe, Y. Prussian blue caged in spongiform adsorbents using diatomite and carbon nanotubes for elimination of cesium. *J. Hazard. Mater.* **2012**, *217–218*, 85–91. [CrossRef] [PubMed]

28. Rad, R.J.; Ghafourian, H.; Asef, Y.; Dalir, S.T.; Sahafipour, M.H.; Gharanjik, B.M. Biosorption of cesium by native and chemically modified biomass of marine algae: Introduce the new biosorbents for biotechnology applications. *J. Hazard. Mater.* **2004**, *B116*, 125–134.

29. Dahiya, S.; Tripathi, R.M.; Hegde, A.G. Biosorption of heavy metals and radionuclide from aqueous solutions by pre-treated arca shell biomass. *J. Hazard. Mater.* **2008**, *150*, 376–386. [CrossRef]

30. Inczedy, J. *Analytical Application of Ions Exchangers*; Pergamon Press: New York, NY, USA, 1966; pp. 348–352.

31. Hayashita, T.; Bartsch, R.A. Competitive sorption of alkali-metal and alkaline-earth-metal cations by carboxylic acid resins containing acyclic or cyclic polyether units. *Anal. Chem.* **1991**, *63*, 1847–1850. [CrossRef]

32. Subramonian, S.; Clifford, D. Monovalent/divalent selectivity and the charge separation concept. *React. Polym.* **1988**, *9*, 195–209. [CrossRef]